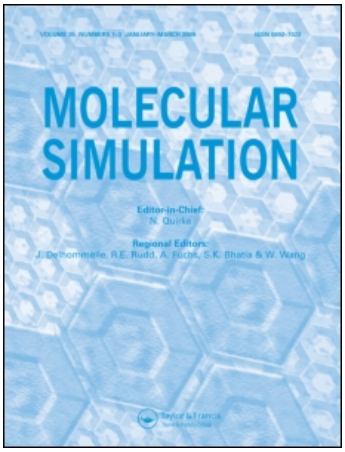

Molecular Simulation
Publication details, including instructions for authors and subscription information:
http://www.informaworld.com/smpp/title~content=t713644482

A Monte Carlo Study of Ring Polymers in Disordered Systems

Dilip Gersappe[ab]; Monica Olvera De La Cruz[a]
[a] Department of Materials Science and Engineering, Robert R. McCormick School of Engineering and Applied Sciences, Northwestern Unversity, Evanston, IL [b] Department of Materials Science and Engineering, University of Pittsburgh, Pittsburgh, PA

To cite this Article Gersappe, Dilip and De La Cruz, Monica Olvera(1994) 'A Monte Carlo Study of Ring Polymers in Disordered Systems', Molecular Simulation, 13: 4, 267 — 283
To link to this Article: DOI: 10.1080/08927029408021993
URL: http://dx.doi.org/10.1080/08927029408021993

Molecular Simulation, 1994, Vol. 13, pp. 267-283
Reprints available directly from the publisher
Photocopying permitted by license only

A MONTE CARLO STUDY OF RING POLYMERS IN DISORDERED SYSTEMS

DILIP GERSAPPE* and MONICA OLVERA DE LA CRUZ

Department of Materials Science and Engineering, Robert R. McCormick School of Engineering and Applied Sciences, Northwestern Unversity, Evanston IL 60208

(Received October 1993, accepted January 1994)

We study the properties of ring polymers in disordered systems using a Monte Carlo algorithm. The algorithm is used to generate a ring on a two dimensional lattice, and the disorder is represented by the random dilution of the lattice. We show how the ring undergoes a cross-over from obeying self avoiding statistics at low concentrations of disorder, to behaving like a branched polymer as the concentration of disorder is increased. We find a scaling behavior to characterize this cross-over phenomenon. We further show how this scaling behavior is also present in another class of problems, namely two dimensional vesicles subjected to a pressure differential.

KEY WORDS: Ring polymers, disorded systems, scaling.

1 INTRODUCTION

The use of Monte Carlo technique to simulate the statistical and dynamic properties of linear polymers has been studied in great detail. There are a variety of schemes to choose from depending on the nature of the simulation [1, 2]. However, methods to study the properties of polymers of different topologies, such as rings, have only recently recieved attention [3–5]. With the discovery of certain DNA in closed circular form, studies on the properties of ring polymers have gained particular significance.

There are a variety of physical situations in which a ring polymer is placed in an inhomogeneous environment, such as a network. For example, in a random network such as a cross-linked polymer gel, this situation arises as a first step in a separation process, such as gel electrophoresis. In a network, the ring is forced into forming a tree-like structure in order to avoid the obstacles [6, 7]. The statistics of a ring now correspond to that of a branched polymer or a lattice animal. The exponent ν, which describes the scaling of the radius of gyration of the ring with the chain length N ($R_g \sim N^{\nu}$), now scales as $5/(2d + 4)$ where d is the spatial dimension [8]. In the absence of a network, the exponent $\nu = \nu_{saw} \sim 3/(d + 2)$. Therefore, the topological interaction of the ring with the network considerably reduces the size of the ring. The behavior of a ring in a random network is thus in direct contrast to that of linear chains, where the

* Present Address: Department of Materials Science and Engineering, University of Pittsburgh, Pittsburgh PA 15261.

exponent ν is unaffected by disorder at least till very close to the percolation threshold of the system [9, 10].

Formulating an analytical treatment of a ring in a network, is associated with a number of problems [6]. The added topological constraint of forming a ring in a network makes the problem fairly intractable. As a result, computer simulations provide an alternate means of studying the problem. In an earlier letter we had reported on the use of a new algorithm to study the properties of ring polymers in disordered systems [11]. In this paper, we supply details of the algorithm that was used and we study how increasing the concentration of disorder induces a change in the statistics of a ring polymer. We will use simple scaling arguments to characterize this behavior.

2 PREVIOUS WORK

On of the first algorithms that was developed specifically for the study of end-restricted polymers such as rings, was the "*bead-jump*" model by Murat and Witten [3]. The "*bead-jump*" scheme involves removing a monomer at a random site along the chain and then reattaching it at another arbitrary point, making sure to satisfy the constraints of self avoidance. In this algorithm, the monomers are displaced considerably from their point of origin. This sort of long-range transport of monomers is referred to as *non-local* moves (*Local* moves on the other hand involve small local perturbations of the chain).

Murat and Witten found that the relaxation time of the polymer scaled as $\tau_R \sim N^3$. However, the actual relaxation times attained by their simulation were 3 to 5 times faster than conventional algorithms (which only have *local* moves), for both linear and ring polymers [3].

A similar algorithm designed for cubic and quadratic lattices was performed by Reiter [4]. In this algorithm, local perturbations of the chains similar to the Verdier-Stockmayer model [1], were combined with *non-local* moves which transport kinks along the backbone or the ring. The algorithm also recovers the N^3 scaling for τ_R seen in the Murat and Witten simulation. Both these algorithms recover the expected scaling for the radius of gyration of the ring with ν, the excluded volume exponent, this being 0.75 in two dimensions [3, 4].

In spite of the progress made in the development of algorithms for the study of the properties of rings, these algorithms have been specifically built for the study of dilute systems. The effect of introducing a ring to a network or any other disordered system has not been taken into account. While the equilibration procedure described in the previous algorithms can be used once the ring is generated inside a network, it does not help us get the initial configuration of the ring.

3 COMPUTATIONAL METHODOLOGY

In the absence of a network, the ring can be started from any arbitrary configuration and the equilibration procedure applied. One could very simply start by generating a random walk and then fold it back on itself to form a ring. This sort of operation is not

possible in a network. The problem with such a technique is that there is a very strong likelihood of the ring being generated in a configuration in which it is stuck and cannot escape. Another method of generating the ring would be to use a variation of the sampling technique for linear chains. As soon as a walk intersects itself the loop that is formed defines the ring. However, there is no way of knowing whether a network point is included in the interior of the ring until all the operations are performed. Computationally, this is a very expensive procedure and as the size of the ring or the concentration of disorder is increased (corresponding to a decrease in the pore size of the gel), it will take a prohibitively long time to grow a ring.

As the generation of the initial conditions of the ring is merely the starting point for the algorithm, it has to be done very efficiently, yet at the same time the ring should be grown in such a configuration in which it is not trapped. To accommodate both these features we have developed an algorithm to grow and equilibrate rings in disordered systems. The algorithm is in two parts, the generation of the initial condition and then the equilibration of the grown ring.

Since we are on a lattice, the final form of the ring is a polygon consisting of N sides. One can sub-divide this polygon into smaller polygons, and continue with this subdivision, until we approach a polygon whose dimensions are the size of the lattice spacing. For example, if we were to grow the ring on a square lattice, the smallest unit that the polygon is composed of would be a square of size axa, where a is the lattice spacing.

We apply this principle in reverse to grow a ring. We start off with the smallest possible unit, a "*primitive cell*". This "*primitive cell*" can be placed anywhere on the lattice as long as its corners do not coincide with a network point. The algorithm proceeds by choosing a side of the first cell and attaching another cell to it, such that the two cells share a common side. (This is what we refer to as a *nearest neighbor* (NN) configuration. A *next nearest neighbor* (NNN) configuration would be one in which two cells share a common corner). The perimeter of the new polygon formed is what defines the ring. Then we choose a cell at random from those which we have placed on the lattice, and try to attach another cell to it in a nearest neighbor configuration. In this manner, we continue attaching cells until the perimeter of the polygon formed reaches the desired value.

The exclusion of the network from the interior of the ring is naturally included in the model, by not allowing the corners of the cells to coincide with the network points. The inclusion of the excluded volume criteria, on the other hand, is a little more complicated. The excluded volume criteria is not satisfied by simply not allowing two cells to occupy the same site, as certain forbidden configurations of the chain result. In particular there are two configurations that violate the excluded volume condition.

In Figure 1a we have one forbidden contact, (two monomers on the same site) and in Figure 1b we have two forbidden contacts. Fortunately, these situations can be easily rectified by the incorporation of two more rules. The first rule is that a cell can have next nearest neighbor *if and only if*, it and its next nearest neighbor share a common nearest neighbor (Fig. 2). The second rule is that no cell can be attached in a configuration in which it has only two nearest neighbors on opposite faces (Fig. 1b).

The ring that is grown can be thought of as being composed of two types of cells, *bulk* cells and *perimeter* cells. Bulk cells have a nearest neighbor count equal to the

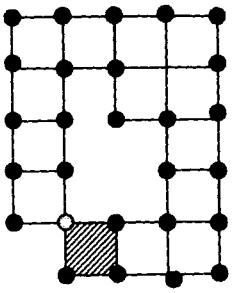

(a)

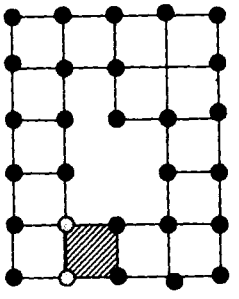

(b)

Figure 1 The violation of the excluded volume constraint. **a** Here we have a pure *NNN* contact. **b** In this case two branches of the ring join together. In both cases the hashed monomers are the ones that violate the excluded volume constraint.

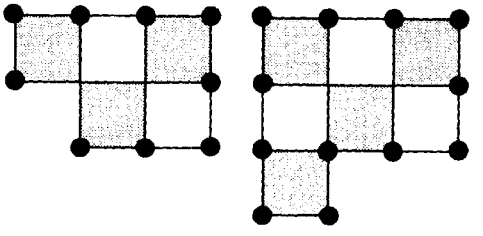

(a) (b)

Figure 2 Allowed Next-Nearest-Neighbor configurations for the primitive cells. In each case the shaded squares are the *NNN*.

coordination number of the lattice. That is, they are surrounded on all sides by other cells. Perimeter cells have a nearest neighbor count less than the coordination number of the lattice and so contribute at least one side towards the perimeter of the polygon.

The perimeter of the polygon at each stage of growth is calculated by a simple formula:

$$N = \sum_{i=1}^{ic} (Z - nn_i) \tag{1}$$

where ic is the total number of cells, Z is the coordination number of the lattice and nn_i is the number of nearest neighbors of cell i.

This algorithm is a very efficient way of generating rings in disordered systems. We have been able to include both the excluded volume condition and the constraint of the network in our algorithm with the formulation of three simple rules. Computationally, these rules are very easy to implement. In order to illustrate the mechanism by which we grow our ring, a typical growth sequence for a ring of size $N = 20$ is shown in Figure 3.

As the ring is grown from these cells in a random manner, i.e. the nth cell is not necessarily attached to the nth cell, the sequence of the N monomers that consititute the perimeter is not stored as a linear function position. That is, we do not know the neighbors of the ith monomer. The connectivity of the monomers however, is maintained by the algorithm.

Once we have our ring generated inside the network we can proceed with the equilibration procedure. We use a method based on the attachment and removal of the "*primitive cells*". For example in Figure 4a corner is flipped, in a manner similar to the

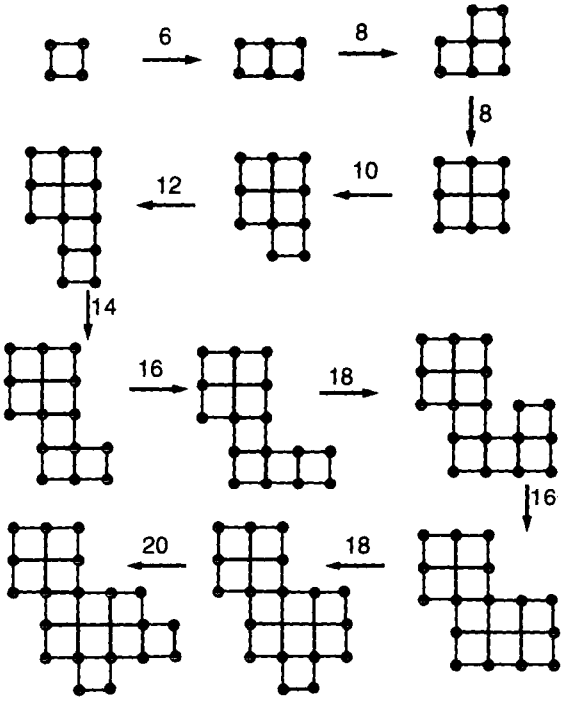

Figure 3 A sequence of events by which a ring size $N = 20$ is grown.

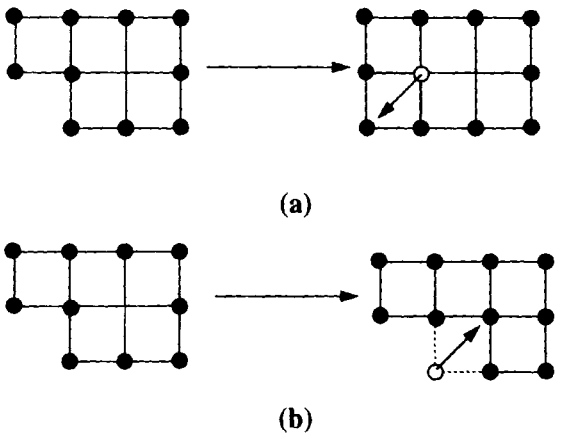

Figure 4 Corner flips in the ring equilibration algorithm.

Verdier-Stockmayer model. The flipping of a corner can be accomplished either by the removal of a cell (Fig. 4a) or by the attachment of a cell (Fig. 4b). These are *one cell* moves, as they involve the movement of one cell, and do not involve a change in the size of the perimeter of the ring.

These moves do not involve long-range transport of the monomers, and are hence local moves. As established by earlier work, on the study of algorithms for the equilibration of rings, local moves are not enough to ensure equilibrium. Long-range transport of monomers is necessary in order for the algorithm to be ergodic [12]. Reiter satisfies this criteria by allowing kinks to move along the perimeter of the ring. In our equilibration scheme this is accomplished by *two cell* moves which proceed as follows. Two types of kinks are possible in our simulation. The first type of kink is a cell attached to just one other cell, i.e. it has a nearest neighbor count of 1. A movement of this cell along the perimeter of the ring involves two steps. The first step is a removal of the cell followed by its reattachment to another cell somewhere along the perimeter or by the removal of a perimeter cell (Fig. 5a). The kink can also exist in another configuration, as shown in Figure 5b. In this case a movement of the kink is accomplished by an attachment of a cell followed by either an attachment or a removal of a perimeter cell. (Fig. 5b)

The only *two cell* moves that do not change the perimeter are the movement of kinks. In our algorithm, the only cells that move are the perimeter cells, but a removal or attachment of a cell causes a change in the status of its nearest neighbors and so a bulk cell can now become a perimeter cell and vice-versa. So, at each step we have to keep track of those cells that constitute the perimeter since that is constantly changing. As the total perimeter of the ring is a constant, we do not expect the number of perimeter cells to fluctuate wildly, but instead expect a fairly peaked distribution about a mean.

In our equilibration procedure we take into account the constraints of the network and excluded volume in the following manner. If a cell is attached, the move is accepted only if there is no network point at the corners of the new square, and if the excluded

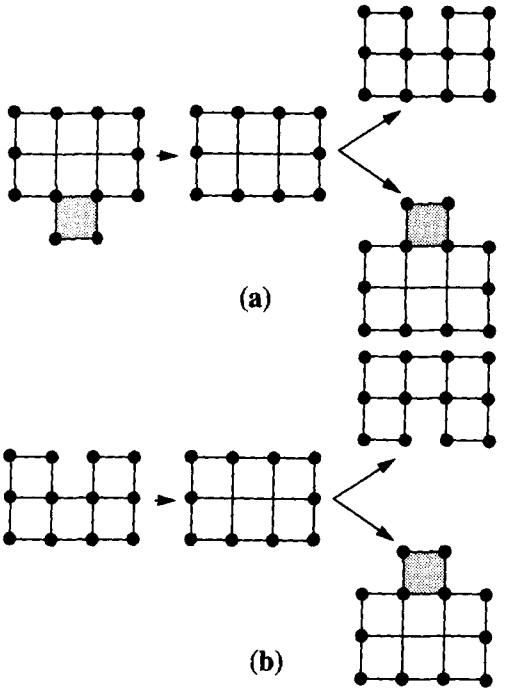

Figure 5 Kink movement in the ring equilibration algorithm. **a** A kink, which is the hashed square, with a nearest neighbor count = 1. **b** Another type of kink, here the kink is inward. In both cases the movement of a kink is accomplished in **two** steps.

volume constraints are met. The rules described earlier in the ring growth algorithm still apply during the equilibration procedure. These rules have to be implemented in a slighly different fashion when a cell is removed. We have to check to make sure that during the removal of the cell we have not introduced any illegal contacts, between its nearest neighbors, which would violate excluded volume constraints.

The algorithm proceeds in the following manner. We first pick up a perimeter cell at random. Then we attempt to move it by choosing a direction at random. If there is another cell present in the direction chosen the move is rejected. Otherwise we choose from a growth or a shrink event. A growth event corresponds to an attachment of a cell, and the shrink event to a removal of cell. So if we pick up a growth event we try and attach another cell to the initial cell that we picked in the direction that we chose. On the other hand, if it is a removal attempt we remove the cell that we picked initially. Next we check the perimeter of the ring to see if there is any change induced by this first step. If there is no change we accept the move, increment the time counter, and continue on by picking up another perimeter cell. If, however, there is a change in the perimeter we allow for a second step, which can restore the perimeter of the ring to its original value. The second step is performed in the exact manner as the first step. If after the end of this second step the perimeter of the ring is restored to its original value, we accept

the move and continue on with the algorithm. However, if the second step fails to restore the perimeter of the ring, the move is rejected and the ring is restored to the condition it was before the first step. The time counter is incremented regardless of whether the second step was successful or not. In this manner we continue with the procedure for a desired number time-steps.

The algorithm requires that we chcek for the change in perimeter after each event. The change in perimeter can be calculated from:

$$N_{\text{change}} = F_i(Z - 2nn_i) \tag{2}$$

where F_i is a flag which is $+1$ for a growth event and -1 for a shirnk event, Z is the coordination number of the lattice and nn_i is the number of nearest neighbors of the ith square on which the operation was performed.

In order to make sure that our equilibration procedure results in true equilibrium the algorithm must be ergodic. That is, the algorithm should be able to sample all possible configurations of the ring. In our algorithm we have two types of moves, one which is a local move similar to the Verdier-Stockmayer model and the second move is one which involves the long-range transport of kinks along the ring perimeter. While we cannot prove the ergodicity of this algorithm exactly, we can show that by the use of this algorithm it is possible to reach a given conformation of the ring starting from an arbitrary initial conformation. In Figure 6 starting from a conformation in which the ring is a straight rod, we show how we can reach a rectangular type conformation in a finite sequence of moves. In a simulation performed on self-avoiding walks (SAW), Caracciolo and Skokal [12] have also demonstrated that these motions, corner flips and long-range transport of kinks, satisfy the principle of ergodicity.

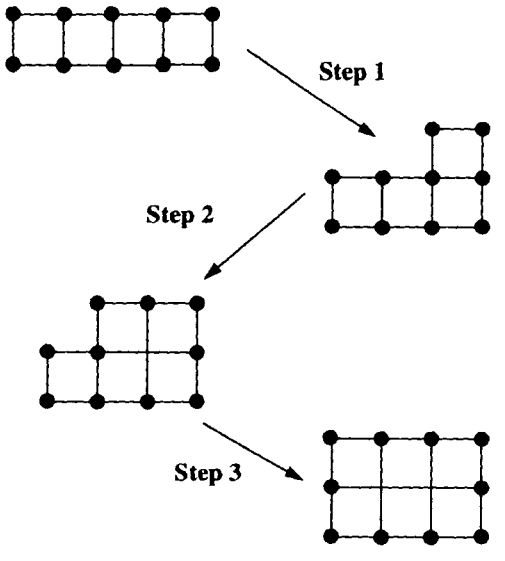

Figure 6 An example of how the movement of perimeter cells transforms the ring from a *rod-like* state to a more *bulky* one.

To ensure that our algorithm produces equilibrium conformations it is sufficient that the principle of detailed balance be obeyed [13]. One of the problems in our simulation is that as the number of *perimeter cells* fluctuate in time, the *a priori* probability of picking one *cell* change correspondingly. This introduces a correction to the detailed balance condition of $1/N_p$ where N_p is the number of *perimeter cells* at a given instant.

4 RESULTS AND DISCUSSION

In order to make sure that our algorithm recovered the correct statistics for the scaling exponent, ν, we ran the simulation for a variety of chain lengths in the absence of disorder. We used a lattice of size 64X64. Periodic boundary conditions were implemented. We grew and equilibrated rings of 20, 40, 60, 80, 100, 120 and 200 links using the algorithm that we described in the previous simulations.

The simulations were first run assuming a relaxation time similar to that observed by Murat and Witten and by Reiter, i.e. $\tau_R \sim N^3$. We ran the simulation for 10^4 Monte Carlo steps, where each Monte Carlo step involved N^3 attempted movements of the ring. Properties of the ring such as the radius of gyration were calculated at the end of each Monte Carlo step.

In Figure 7 we show the scaling of the radius of gyration of the ring, in the absence of disorder, as a function of the chain length, N. The exponent, ν, that describes the radius

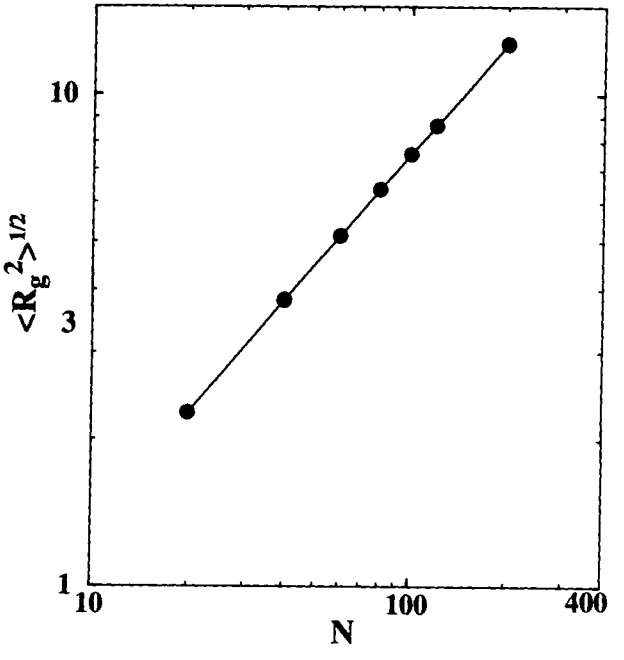

Figure 7 Scaling of the radius of gyration of a ring, R_g with chain length, N, in the absence of disorder. The scaling exponent, $\nu = 0.745 \pm 0.006$.

of gyration scaling was found to be 0.745 ± 0.006 in excellent agreement with theoretical predictions as well as the previous simulations on this system [3, 4].

In spite of the agreement of the simulation results with previous work, there is still the deviation from the detailed balance condition as discussed earlier. As this is directly as a result of the fluctuations in the number of perimeter cells that constitute the ring, we kept track of the number of perimeter cells as a function of time for different chain lengths, to make sure that the deviation was within acceptable limits (Fig. 8). As can be seen from this figure, the number of perimeter squares is a fairly well behaved function in time, with oscillations about a mean value, $\bar{N}_p$.

While these plots are strong indicators that our algorithm does indeed produce equilibrium structures, there is another quantity that one can measure which would also serve as a test for the algorithm. It has been conjectured that in the absence of any disorder, the area enclosed by the ring should scale with the radius of gyration of the ring as [14]:

$$\text{Area} \sim [R_g^2] \sim N^{2\nu}. \tag{3}$$

In our algorithm the area enclosed by the ring is simply equal to the total number of cells that comprise the ring. The scaling behavior of the area of the ring is shown in Figure 9, where the exponent ν' that describes the scaling is equal to $2\nu \pm 0.007$.

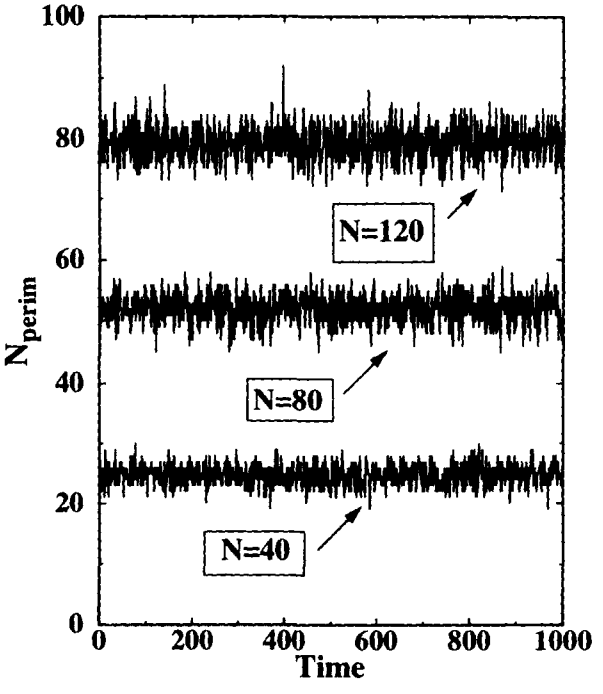

Figure 8 The number of perimeter squares, N_{perim} as a function of time for three different ring lengths, N, in the absence of disorder.

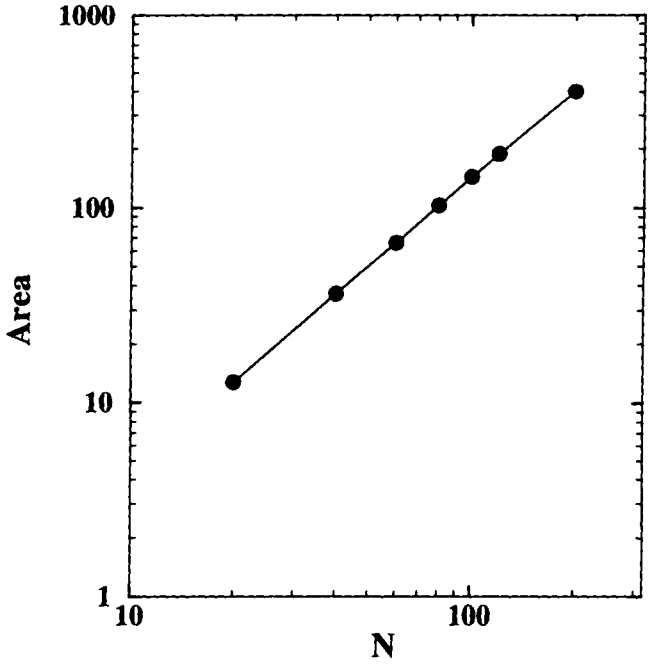

Figure 9 Plot of the area enclosed by the ring vs. ring size, N. The scaling exponent was found to be $2\nu \pm 0.007$.

While the most severe test of any algorithm is to make sure that it produces equilibrium structures, it is also essential that it should be as efficient as possible. In performing a Monte Carlo simulation, to avoid statistical errors, averages over equilibrium states have to be taken over times larger than the times over which these states are correlated. The time between two statistically independent states of the system is defined as the relaxation time, τ_R. Thus, in order to design an efficient algorithm, the relaxation time of the system has to be minimized.

One of the methods used to identify the relaxation time in polymeric simulations is to say that the polymer has relaxed when it's center of mass has moved a distance equal to its radius of gyration [3]. Using this definition for the relaxation time, τ_R, we ran the simulations for a variety of chain lengths, keeping track of the number of moves necessary for the polymer to diffuse a distance equal to its radius of gyration. From our simulation we found that the relaxation time scaled as $\tau_R \sim N^{2.25}$ where N is the length of the chain. In the Murat and Witten algorithm, as well as the Reiter algorithm, relaxation times that scaled as N^3 were observed in spite of the "*global moves*" that were incorporated. The reason for this slow down was because the "*global moves*" in the algorithm were correlated and consequently were unable to relax local perturbations. In our algorithm the movement of the monomers of the ring is accomplished by the movement of our *primitive cells*. Since the movement of these *cells* are essentially independent of each other, we would expect that the slow down in the relaxation time seen in the previous algorithms would not be seen here.

Using this estimate for our relaxation time we then proceeded to calculate the properties of our rings in the presence of a random network. We introduced the network into our system by picking up points at random from an MXM integer array and then placing these points on a lattice of the same dimensions. We used a lattice of size 64X64 and implemented periodic boundary conditions.

Before the ring growth algorithm was started, we first used a standard cluster counting algorithm, to identify the infinite cluster. The ring was seeded on this cluster, i.e. the first *primitive cell* was placed on this cluster. The ring was then grown and equilibrated on this cluster. The ring was given $5N^2$ movements to equilibrate after which properties of the ring were calculated at the end of each Monte Carlo step where each step involved $5N^2$ movements of the ring.

The concentrations of disorder that were used were in the range of $p = 0.02$ to $p = 0.12$, where p is defined as the fraction of sites on the lattice that are occupied by impurities. Chains of length $N = 20, 40, 60, 80, 100$ and 120 were used. The simulations were run for 10^5 Monte Carlo steps and the results were then averaged over 5 different realizations of the disorder.

The first effect that we were looking for was the behavior of the radius of gyration of the chain as a function of the concentration of disorder. One can in fact speculate, by means of a scaling argument, how the disorder would affect the statistics of the chain. We know that as the concentration of disorder is increased, the ring undergoes a transition from a self-avoiding walk to a lattice animal, with the radius of gyration scaling with the chain length N as $R_g \sim N^{\nu_{LA}}$ is the lattice animal exponent, this being 0.64 in two dimensions [8].

We can determine the scaling factor of the radius of gyration with the concentration of disorder, by use of a scaling argument. The characteristic length scales that enter the picture are R_0, the unperturbed radius of gyration of the chain, and the length scale of the disorder, which is denoted by ξ. We can then write [12]:

$$R_g^2(p, N) = R_0^2 \phi_r\left(\frac{R_0^2}{\xi^2}\right) \tag{4}$$

where ϕ_r is a dimensionless function. In our model, the length scale, ξ is simply the distance between impurities. ξ scales with impurity concentration as $\xi \sim 1/p^{1/d}$ where d is the spatial dimension and p is the fraction of sites on the lattice occupied by obstacles. R_0 is the unperturbed Flory radius of gyration of the chain ($R_g \sim N^{\nu}$). Therefore, substituting in equation (4) we get

$$R_g^2(p, N) = R_0^2 \phi_r(pN^{2\nu}). \tag{5}$$

In the limit of $pN^{2\nu} \gg 1$ we can expand $\phi_r(x) \sim x^{\alpha}$. Since in this limit we have $R_g \sim N^{\nu_{LA}}$ and $R_0 \sim N^{\nu}$, we have

$$\alpha = (\nu_{LA} - \nu)/\nu. \tag{6}$$

We can also recover this expression determine by the use of a *blob* argument. We assume that in the limit of large N we can subdivide our ring into blobs of size ξ, with each blob having n_b monomers in it. A schematic representation of our ring of blobs is shown in Figure 10. Inside each blob as the effects of the boundary are weak, the ring still obeys self-avoiding statistics, i.e. we have $\xi \sim n_b^{\nu}$ with $\nu = 0.75$ in two dimensions.

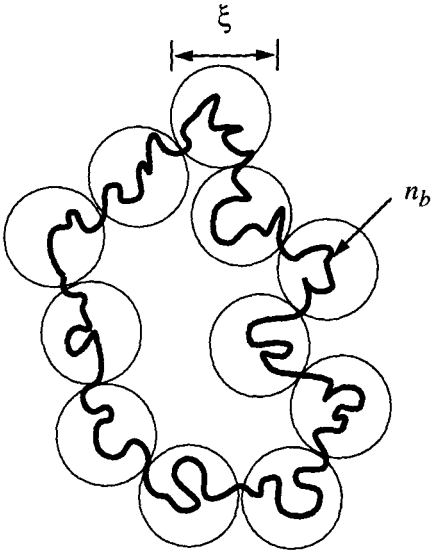

Figure 10 A ring denoted by the solid line is now covered with blobs of size ξ. Each blob has n_b monomers of the ring. The blobs are the solid circles that cover the ring.

Now we can express the radius of gyration of the ring in terms of these *blobs* in the following manner. As our new ring of *blobs* obeys lattice animal statistics we have

$$R_g^2 \sim N_{\text{blob}}^{2\nu_{LA}} \xi^2 \tag{7}$$

where N_{blob} is the number of *blobs* given by $N_{\text{blob}} = N/n_b$

The size of the blob ξ is also related to the concentration of disorder in the same manner as before, i.e. $\xi \sim (1/p)^{1/d}$. Substituting, we have

$$R_g^2 \sim \left(\frac{N}{n_b}\right)^{2\nu_{LA}} \frac{1}{p}. \tag{8}$$

Now substituting for n_b and on further simplification we have

$$R_g^2 \sim N^{2\nu_{LA}} p^{(\nu_{LA}-\nu)/\nu}. \tag{9}$$

This is exactly the same expression we had derived earlier by use of our scaling argument.

Plots of $R_g^2/N^{2\nu}$ vs. $pN^{2\nu}$ will serve to test the scaling hypothesis that we have postulated. This can be seen in Figure 11 where curves for different N's and concentrations of disorder collapse to a single curve, thus confirming our scaling variable. The coefficient α can be determined from this plot, and we found that $\alpha = -0.1217 \pm 0.02$, [11] in excellent agreement with the theoretical predictioins. Using this value to back calculate for the lattice animal exponent we get $\nu_{LA} = 0.654 \pm 0.02$. The error bars on the calculation of α are large mainly due to finite size effects. We have to use fairly large intervals when we want to compare results of different concentrations of disorder, as

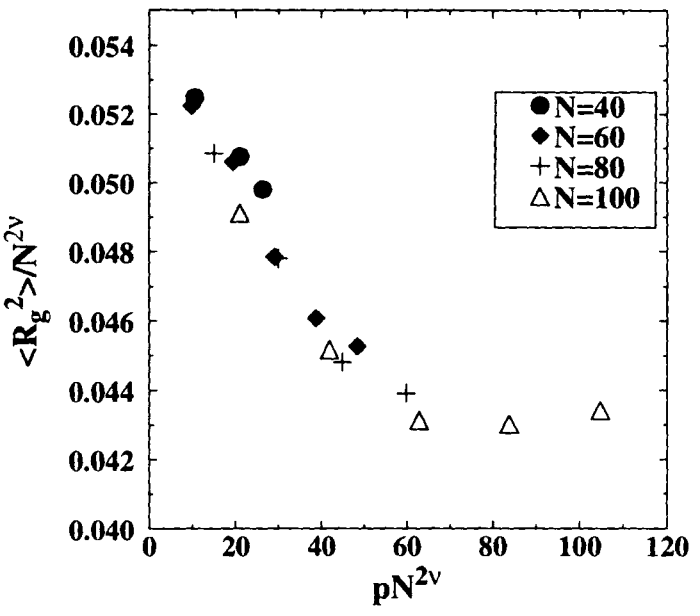

Figure 11 Scaling plot for the radius of gyration of the chain for different chain lengths, N and different concentrations of disorder p.

subtle changes in the concentration of disorder are not picked up by this small system size.

To make sure that the ring had equilibrated we kept track of the movement of the center of mass of the ring and checked to see if the ring had sampled the entire lattice. However, as the concentration of disorder was increased, or if we used a larger ring, the diffusion of the ring showed down rather dramatically. This imposed a practical limitation on the size of the rings and the concentration of disorder that we could analyze through our algorithm.

In spite of this limitation the scaling laws that have been postulated seem to be borne out quite nicely by the simulation. The behavior of rings in disordered systems is thus in direct contrast to that of linear chains. While the exponent ν is unaffected for linear chains, at least till very close to the percolation threshold, the added effect of the topology of the ring, induces a transition of the ring from self avoiding to lattice animal statistics.

This sort of behavior has also been observed in a related study on the effect of pressure on two-dimensional vesicles [16]. Leibler *et al.* modeled the vesicle as a two dimensional off lattice ring of N beads, each of diameter a. A pressure difference, Δp, was introduced between the interior and the exterior of the vesicle.

While they analyzed the effect of both a negative and a positive Δp on the statistics of the ring, the one that is analogous to our simulation is when the pressure on the exterior of the vesicle is larger than the pressure inside the vesicle. This region has been dubbed the "*deflated regime*".

They found that in this regime the radius of gyration of the ring underwent a transition from self-avoiding statistics to a branched polymer or a lattice animal. They used a standard Metropolis algorithm consisting of local bead moves to equilibrate their system. The self-avoidance criteria was implemented by only allowing very small Monte Carlo steps.

To find out the scaling relationship between the radius of gyration and the pressure differential, they postulated that the radius of gyration of the vesicle and the area enclosed by the vesicle should be of the form

$$R_g^2 \sim N^{2\nu} X(\bar{p} N^{\phi\nu}), \quad A \sim N^{2\nu_A} Y(\bar{p} N^{\phi\nu}) \tag{10}$$

where ν is the standard self-avoiding exponent, and $\nu_A = \nu$ as established by earlier work and

$$\bar{p} = (\Delta p a^2)/(k_B T) \tag{11}$$

where a is the diameter of the beads that consititute the vesicle [16]. In order to determine ϕ they set $\Delta p = 0$ and studied the variations of the area, A, and its fluctuations. They found that

$$(\Delta A)^2 \equiv \langle A^2 \rangle - \langle A \rangle^2 = \frac{\partial A}{\partial \bar{p}} \sim N^{2\nu_A + \phi\nu}. \tag{12}$$

Using this they calculated the value of ϕ and found that $\phi = 2.13 \pm 0.17$. In our simulation, the analog of the pressure differential is the concentration of disorder, p. If we perform a similar analysis on our system, i.e. set the concentration of disorder to zero, and study the fluctuations in the total number of *cells* that comprise the ring, we

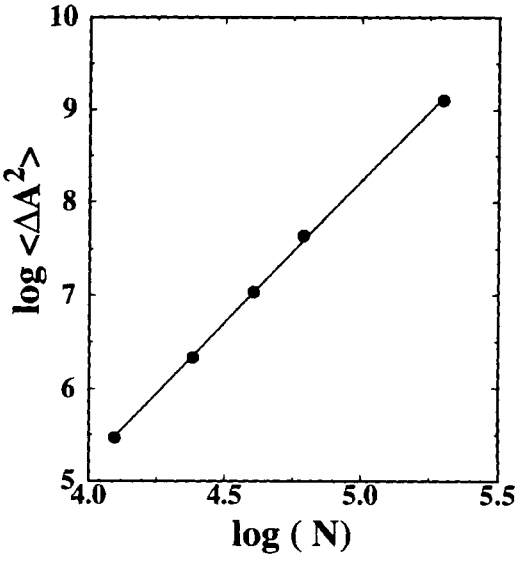

Figure 12 Scaling of the fluctuation in area $\langle A^2 \rangle$ with the chain length N. The exponent determined from the line of best fit was 2.03 ± 0.008.

should also be able to recover the scaling exponent that we had postulated earlier. This is shown in Figure 12 where fluctuations in the area are plotted vs. the chain length. The exponent ϕ was found to be 2.03 ± 0.008.

The exponent for the power low scaling of the radius of gyration of the vesicle, α was found by Leibler *et al.* to be -0.13 ± 0.05 which is very similar to what comes out of our simulation. All this indicates that a ring trapped inside a random (quenched) environment can be mapped onto the problem of a two dimensional vesicle with a pressure difference between the interior and the exterior of the vesicle.

In addition to the radius of gyration scaling, the area enclosed by the ring should also scale in the same manner as the vesicle. The scaling of the area enclosed by the ring with the concentration of disorder and the ring size is shown in Figure 13, where once again the curves for different N's collapse to a single curve. Thus, the analogy is complete with the pressure difference being replaced by the concentration of disorder. It should be noted that the analogy that we have developed between the two systems is a result of the coincidence of the results that come out of the simulations. We are unable to draw a rigorous mathematical analogy between the two systems.

5 CONCLUSIONS

In conclusion we have demonstrated that the effect of introducing the topological constraint of forming a ring in a fixed disordered network, introduces a whole new

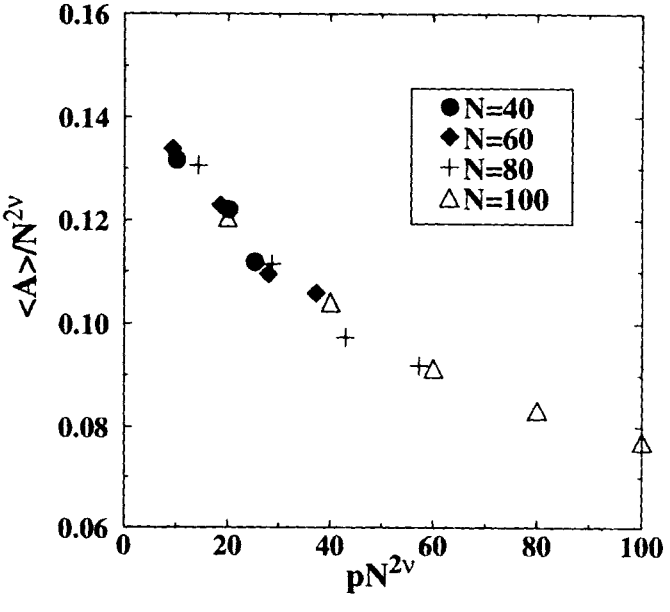

Figure 13 Scaling Plot for the area enclosed by the ring for different chain lengths, N and different concentrations of disorder p.

series of interesting properties. The ring polymer reacts to an increase in the concentration of disorder by changing from obeying self-avoiding statistics to a form in which it is like a lattice animal or a branched polymer. Both the radius of gyration and the area enclosed by the ring can be described by very simple scaling relationships, which show the interplay between the chain length and the concentration of disorder. The problem is shown to map into one in which a two dimensional vesicle is subjected to a pressure difference between the interior and the exterior of the vesicle.

Acknowledgements

We would like to thank B. Duplantier and J. M. Deutsch for valuable discussions. M. O. would like to thank the financial support from the Lucille and David Packard Foundation. This was supported in part by NSF grant no DMR 9057764 and by a grant from the National Institutes of Health.

References

[1] P. Verdier and W. H. Stockmayer, "Monte Carlo calculations on the dynamics of polymers in dilute solution", *J. Chem. Phys.*, **36**, 227 (1962).
[2] N. Madras and A. Skokal, "The Pivot Algorithm: A highly efficient Monte Carlo method for the self-avoiding walk", *Journal of Statistical Physics*, **50**, 109 (1988).
[3] M. Murat and T. Witten, "Relaxation in bead-jump polymer simulations", *Macromolecules*, **23**, 23 (1990).
[4] J. Reiter, "Monte Carlo simulations of linear and cyclic chains on cubic and quadratic lattices", *Macromolecules*, **23**, 3811 (1990).
[5] A. Romero, "A simple model for the shape of vesicles in two dimensions", *Journal de Physics I*, **2**, 15 (1992).
[6] M. E. Cates and J. M. Deutsch, "Conjectures on the statistics of ring polymers" *Journal de Physique*, **47**, 2121 (1987).
[7] M. Rubenstein, "Dynamics of ring polymers in the presence of fixed obstacles", *Phys. Rev. Lett.*, **57**, 3023 (1986).
[8] J. Isaacson and T. C. Lubensky, "Statistics of lattice animals and dilute branched polymers", *J. Phys. (Paris)*, **41**, L469 (1980).
[9] S. B. Lee and H. Nakanishi, "Self-avoiding walks on randomly diluted lattices", *Phys. Rev. Lett.*, **61**, 2022 (1988).
[10] D. Gersappe, J. M. Deutsch and M. Olvera de le Cruz, "Density fluctuations of self-avoiding walks in random systems", *Phys. Rev. Lett.*, **66**, 731 (1991).
[11] D. Gersappe and M. Olvera de le Cruz, "Ring macromolecules in topologically restricted environments", *Phys. Rev. Lett.*, **70**, 461 (1993).
[12] S. Caracciolo and A. Skokal, "Dynamic critical exponent of some Monte Carlo algorithms for the self-avoiding walk", *J. Phys. A: Math. Gen.*, **19**, L797 (1986).
[13] K. Binder (Ed.), *Monte Carlo Methods in Statistical Physics*. Springer-Verlag, 1979.
[14] M. E. Fisher, "Fractal and non-fractal shapes in two-dimensional vesicles", *Physica D*, **38**, 112 (1989).
[15] P. de Gennes, *Scaling Concepts in Polymer Physics*. Cornell Univ. Press, 1979.
[16] S. Leibler, R. Singh, and M. E. Fisher, "Thermodynamics of two dimensional vesicles", *Phys. Rev. Lett.*, **59**, 1989 (1987).